Cent. Eur. J. Chem. • 10(2) • 2012 • 395-406
DOI: 10.2478/s11532-011-0162-z

VERSITA

Central European Journal of **Chemistry**

Theoretical investigation of the Anti-Parkinson drug rasagiline and its salts: conformations and infrared spectra

Research Article

U.Ceren Başköse[1], Sevgi Haman Bayarı[2], Semran Sağlam[1], Hacı Özışık[3]

[1]*Gazi University, Faculty of Arts and Science, Physics Department, 06500 Teknikokullar, Ankara, Turkey*

[2]*Hacettepe University, Faculty of Education, Physics Department, 06800 Beytepe, Ankara, Turkey*

[3]*Aksaray University, Arts and Science Faculty, Physics Department, 68100 Aksaray, Turkey*

Received 15 August 2011; Accepted 12 December 2011

Abstract: The conformational analysis of rasagiline [*N*-propargyl-1(*R*)-aminoindan] was performed by the density functional theory (DFT) B3LYP method using the 6-31++G (d,p) basis set. A single point energy calculations based on the B3LYP optimized geometries were also performed at MP2/6-31++G (d, p) level. The vibrational frequencies of the most stable conformer of rasagiline was calculated at the B3LYP level and vibrational assignments were made for normal modes on the basis of scaled quantum mechanical force field (SQM) method. The influence of mesylate and ethanedisulfonate salts on the geometry of rasagiline free base and its normal modes are also discussed.

Keywords: *Rasagiline • Conformational analysis • Rasagiline salts • DFT • Infrared*

1. Introduction

Rasagiline, the R(+) enantiomer of n-propargyl-1-aminoindane, is an active substance of azilect that is used to treat Parkinson's disease. It is in a class of medications called monoamine oxidase (MAO) type B inhibitors [1]. The S-enantiomer of rasagiline is less active on MAO [2]. The exact mechanism of action of rasagiline is unknown. One mechanism is believed to be related to its MAO-B inhibitory activity, which causes an increase in dopamine levels and activity in the brain that affects motor function. Rasagiline improves motor function, which is affected by Parkinson's disease.

AZILECT® tablets contain rasagiline mesylate. Rasagiline salts are more storage-stable than rasagiline free base in solid medicinal products. The mesylate salt of rasagiline [(R)-N-2-Propynyl-1-indanamine methanesulfonate] is freely soluble in water [3]. The other salt of rasagiline ethanedisulfonate (edisilate) [bis[(1R)-N-prop-2-ynyl-2,3-dihydro-1H-inden-1-aminium] ethanedisulfonate] can be stored under humid conditions [4]. The crystal structure rasagiline ethanedisulfonate has been reported by Bruning *et al*. [5].

The properties of active substances in pharmaceutical drugs are very important. However, despite its pharmaceutical importance, to the best of our knowledge, no structural, conformational, vibrational or theoretical studies for rasagiline have been published. In this manuscript, a conformational and vibrational study of rasagiline was performed using quantum mechanical density functional theory (DFT) calculations.

The primary goal of this work was to obtain the most stable conformer of rasagiline and assignment of the vibrational spectra of this structure. To estimate the electron correlation effects that cannot be partially included in the DFT calculations, single-point MP2 energy

* *E-mail: bayari@hacettepe.edu.tr*

calculations were performed at the geometries obtained in the B3LYP calculations with the same basis set.

The experimental wavenumbers of rasagiline were taken from [6]. The complete assignments were performed on the basis of the total energy distribution (TED) of the vibrational modes, calculated with scaled quantum mechanics (SQM) method [7,8]. DFT calculations were also performed for rasagiline mesylate and rasagiline ethanedisulfonate salts to provide theoretical support for the structural and vibrational properties of rasagiline salts.

2. Computational details

All calculations were performed on a Linux machine using the Gaussian 03W quantum chemistry package [9].

The relaxed potential energy surface (PES) scan for dihedral angle τ_1(7-8-10-11), was carried out at every 10° interval with the range of 0-180° at the DFT/B3LYP/6-31++G(d,p) level [10,11]. The relaxed PES calculations were also performed for dihedral angle τ_2 (7-8-10-23) and τ_3 (8-10-11-12)] values in the same range (Fig. 1).

The structures corresponding to the minima in the each PES were further optimized at the B3LYP/631++G(d,p) and MP2/631++G(d,p) levels. MP2/631++G(d,p) single point energy calculations at the B3LYP geometries were also performed. The relative conformer abundances were calculated according to Boltzmann distribution at 298.15 K.

A vibrational analysis was performed on all DFT structures to insure the absence of negative vibrational frequencies and verify the existence of a true minimum. The harmonic and anharmonic frequencies of most stable structure of rasagiline free base were calculated. The vibrational assignments were made on the basis of the total energy distribution (TED) calculated with scaled quantum mechanics (SQM) method [7,8] based on DFT calculation. The total energy distributions (TED %) of the vibrational modes were calculated with the SQM program (Windows version 1.0) [12]. The animation option of the Gauss View 03W graphical interface for Gaussian programs was also used for the assignment of the calculated wavenumbers.

The initial geometrical parameters of rasagiline ethandisulfonate salt were obtained directly from the crystal data [5] and reoptimized at the B3LYP/6-31++G(d,p) level. The rasagiline mesylate anion structure was also optimized, and the harmonic frequencies of the rasagiline salts were calculated.

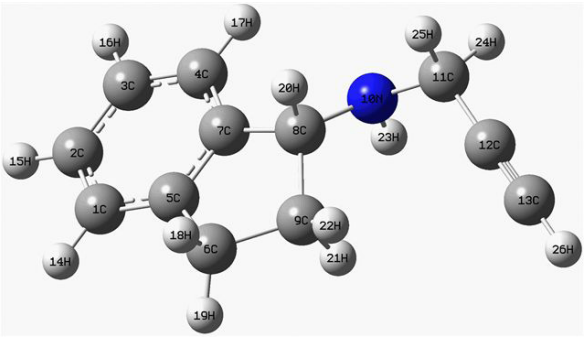

Figure 1. Molecular structure and atom numbering scheme of rasagiline

3. Results and discussion

3.1. Conformational study

Molecular conformation plays a crucial role in the function and selectivity of flexible molecules of biological interest. It has been reported that solid rasagiline free base, rasagiline mesylate, and rasagiline ethanedisulfanate have no known polymorphs [5,6,13]. Rasagiline possesses an indane ring, an -NH group, and a propargyl chain (Fig. 1). Indane and its derivatives are components of many biological molecules. It is composed of a benzene ring fused with a saturated five-membered ring. The substitution of the five-membered ring of indane gives rise to several conformers [14]. The structure-activity relationship among rasagiline-related compounds suggests the crucial role of the propargyl moiety in these molecules [2,15].

To understand the conformational preferences of the rasagiline free base, DFT calculations were performed in the gas phase. The calculations were only performed on the R enantiomer of rasagiline. To express the energy as a function of the dihedral angles around three rotatable bonds, angles τ_1(C7-C8-N10-C11), τ_2 (C7-C8-N10-H23) and τ_3 (C8-N10-C11-C12) were selected (Fig. 1). The orientation of NH group and the propargyl group with respect to the ring were represented by τ_2 and τ_3, respectively.

The computations reveal eight minima. The relative energies ΔE (kcal mol^{-1}), zero point energy corrected relative energies, dihedral angles for the most relevant conformers electric dipole moments (D), and the Boltzmann populations of the conformers at the B3LYP/ 6-31++G(d,p) level of theory are given in Table 1. For comparison MP2/6-31++G (d,p) results are also given in the same table.

Fig. 2 shows eight DFT conformers of rasagiline. Although **I** is the energetically most stable conformer, conformer **II** is also energetically close to **I** (less than 0.2 kcal mol^{-1}). The calculated infrared spectra in the range 2100-3100 cm^{-1} and below 500 cm^{-1} are different

Table 1. The Relative energies (kcal/mol), dihedral angles (°), dipole moments (D) and populations (%)of the rasagiline [a]

Conf.	B3LYP		MP2		B3LYP/MP2				
	ΔE	ΔE ZPEcorrected[b]	ΔE (Single Point)	ΔE (OPT)	τ_1 (7-8-10-11)°	τ_2 (7-8-10-23)°	τ_3 (8-10-11-12)°	μ(D)	P[c]
I	0	0	0	0	166.6/169.4	-65.0/-63.2	72.0/69.7	0.858/1.036	29.3
II	0.158	0.182	0.740	0.835	175.6/-178.4	-59.60/-57.4	179.4/179.4	1.498/1.657	22.5
III	0.266	0.278	0.010	0.012	66.7/64.4	-170.5/-173.5	58.9/56.4	0.801/0.914	18.8
IV	0.523	0.625	0.453	0.465	177.9/177.4	-58.9/-56.5	-67.8/-63.6	1.478/1.593	12.2
V	0.542	0.547	0.021	0.047	171.4/174.2	48.2/55.5	-61.5/-63.6	0.613/0.816	11.8
VI	1.239	0.591	0.546	0.578	-67.9/-67.9	162.6/166.1	-85.7/-83.8	0.971/1.128	3.7
VII	1.782	1.872	1.486	1.467	-49.8/-50.7	76,30/71.9	171,7/161.5	1.072/1.195	1.5
VIII	2.712	2.568	3.140	3.210	93.9/92.9	-143,8/-145.1	171,1/171.2	1.537/1.674	0.3

[a] *All relative energies were calculated with respect to conformer I.*
[b] *ZPE-corrected relative energies using the vibrational wavenumbers obtained at the same level of theory as the geometry optimization*
[c] *Population from ΔE (DFT/B3LYP) taking T = 298.16 K*

for conformers **I** and **II**. The dipole moment values of these conformers are also different (Table 1). Likewise, conformers **IV** and **V** are energetically close, but their dipole moment values are different due to the different orientation of the -NH group in each conformer. Note that the infrared spectra of conformer **V** in the amide N-H stretch region provide a striking contrast to those of **IV**.

The DFT/B3LYP is widely used for the conformational analysis and theoretical vibrational frequency calculations with reasonable correlation with experimental results [16-18]. However the B3LYP functional do not cover the dispersion energy and dispersion effects, which may play a role in the conformational stability of aromatic organic molecules. It is generally thought that relative energies are more sensitive to the level of theory applied than molecular geometries. A number of recent combined experimental/computational studies on gas-phase molecules use this method of DFT geometry optimization followed by MP2 single-point calculation [19-21]. A comparison of the relative energies calculated at the optimized geometry at the B3LYP/6-31++G(d,p) level, including ZPE-corrected relative energies, and the single point calculations at the MP2/6-31++G(d,p) indicate some differences in the predicted conformational ordering.

As can be seen from Table 1 conformer I is also the most stable conformer according to the MP2 calculations. However, the energy gap between conformer I and conformers III/V almost disappears at the MP2/6-31+G (d, p) level. The significant change at the MP2 level was also found in the other studies [22-25]. The B3LYP generally underestimate the strength of interactions with π electron clouds [26]. It is also well established that the MP2 method performs extremely well for hydrogen-bonded systems [27]. The observed discrepancies between the MP2 and DFT relative stability of conformers may indicate that also in this case.

The bond lengths vary little with the conformations (geometric parameters and calculated spectra of all conformers are available from the authors upon request). For all structures, the propargyl C(11)-C(12)-C(13) angle is nearly 180°. The *trans*-propargyl was identified as the most stable conformation labeled **I.** In conformational studies of N-methylpropargyl amine by microwave spectroscopy [28], one conformer [lone pair trans to the ethynyl group] was observed in the solid phase. Ab initio calculations [29] also indicate this conformer (LP-trans) as the most stable in the gas phase. Similar to propargyl amine, the repulsion between the π-electrons of the triple bond and the lone pair electrons of nitrogen might provide a more stabilized structure in rasagiline.

The MP2 and B3LYP optimized geometry of the most stable conformer is in a good agreement with each other. In this paper we discuss both geometries and vibrational frequencies obtained at the B3LYP level.

3.2. Structural properties

Table 2 summarizes the selected structural parameters for the most stable conformer of rasagiline in accordance with the atom-numbering scheme in Fig. 1. Because the experimental structure of this molecule is not available, the optimized structure can only be compared with the crystallographic structures taken from rasagiline ethanedisulfonate salt [5]. Therefore, we also calculated the geometric structures of rasagiline ethanedisulfonate and rasagiline mesylate (azilect) salts (Fig. 3a and 3b, respectively). Table 2 also includes the optimized structural parameters of these rasagiline salts.

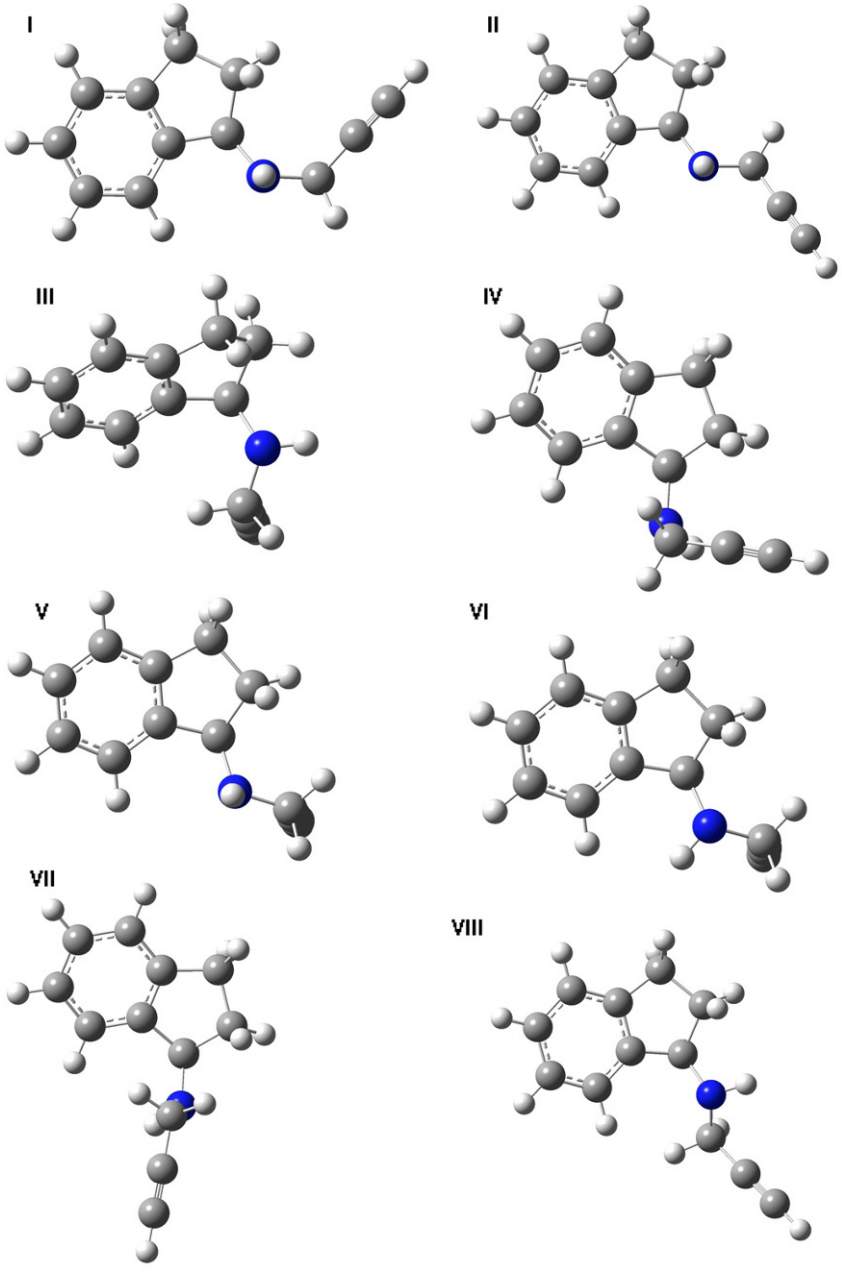

Figure 2. Fully optimized structures calculated at B3LYP/6-31++G(d,p) of the eight conformers of rasagiline.

In the calculated structure of rasagiline, the benzene ring shows planarity, and the five-membered ring shows a conformation that appears like an envelope similar to that of the crystal structure of rasagiline ethanedisulfonate. All of the C-C bonds of the benzene ring are equivalent (ca. 1.40 Å). The calculated C-C bond lengths in the five-membered ring range from 1.51-1.56 Å, and the ring C-H distances range from 1.086–1.101 Å. All bond lengths and angles are within normal ranges. The calculated C_{indane}-N and $C_{propargyl}$-N bond lengths of rasagiline are shorter than the corresponding bonds of rasagiline ethandisulfonate and rasagiline mesylate (Table 2).

The propargyl moiety has triple and single C-C bonds. In rasagiline, the triple bond length (C12≡C13) and single bond length (C11–C12) are calculated as 1.211 Å and 1.477 Å, respectively. These bond lengths of rasagiline are longer than those of its salts. The structural parameters calculated for the propargyl group of rasagiline agree well with the experimental microwave data for propargyl fluoride [30].

Table 2. The selected optimized geometric parameters of rasagiline, rasagiline ethanedisulfonate and Rasagiline mesylate.

Geometric parameters	Rasagiline salts		Rasagiline	Exp.[b] Ras.ethandisul.
	Ethanedisulfonate	Mesylate [a]		
Bond lengths (Å)				
C(2)-C(3)	1.399	1.399	1.400	1.377
C(5)-C(6)	1.512	1.512	1.514	1.498
C(7)-C(8)	1.519	1.520	1.521	1.500
C(8)-N(10)	1.506	1.501	1.461	1.514
N(10)-C(11)	1.509	1.507	1.463	1.485
N(10)-H(23)	1.017	1.024	1.017	0.920
C(11)-C(12)	1.458	1.458	1.477	1.462
C(12)≡C(13)	1.208	1.208	1.211	1.164
C(13)-H(26)	1.067	1.066	1.066	0.949
S_{28}-O_{29}	1.474	1.473 (1.458)[a]		1.426
S_{28}-O_{27}	1.530	1.513 (1.458)		1.442
S_{28}-C_{30}	1.823	1.797 (1.757)		1.804
C_{30}-C_{34}	1.522			
N_{10}....O_{27}	2.596	2.552		2.755
Bond Angles (˚)				
C(1)-C(2)-C(3)	120.6	120.4	120.4	121.4
C(6)-C(5)-C(7)	110.8	110.7	110.4	111.2
C(5)-C(7)-C(8)	109.5	109.5	110.8	109.8
C(6)-C(9)-C(8)	104.6	104.6	105.2	105.2
C(7)-C(8)-N(10)	112.2	112.3	112.1	111.4
C(8)-N(10)-C(11)	117.3	117.3	117.2	114.3
N(10)-C(11)-C(12)	114.8	114.4	117.3	110.2
C(11)-C(12)- C(13)	176.9	177.0	178.3	177.8
O_{27}-S_{28}-O_{29}	110.0	109.1		110.7
O_{27}-S_{28}-O_{41} or $O_{34\ mesylate}$	113.2	112.1 (112.0)		113.5
O_{27}-S_{28}-C_{30}	103.1	103.5 (106.7)		109.6
S_{28}-C_{30}-C_{34}	109,4			109.5
Dihedral Angles (˚)				
C(7)-C(5)-C(6)-C(9)	-17.6	-17.7	-17.0	13.3
C(6)-C(5)-C(7)-C(4)	-177.7	-178.0	-179.3	-176.5
C(5)-C(6)-C(9)-C(8)	27.5	27.8	27.2	-23.6
C(4)-C(7)-C(8)-N(10)	-40.7	-39.7	-35.5	-80.7
S (28)-C(30)-C(34)-S(37)	-178.6			-139.2
H(35)-C(34)- C(30)H(32)	58.4			
Energy (Hartree)	-1846.62729	-1184.173566	-519.817805	

[a,b] *Taken from [31] and [5], respectively.*

In the solid state structure [5], ethanedisulfonate anions ($C_2H_4O_6S_2^-$) are connected by N-H….O hydrogen bonds to rasagiline cations, which give structural stability. The five-membered ring has a conformation close to that of an envelope. Both H atoms of the $–NH_2^+$ group of the rasagiline cation are involved in hydrogen bonding. The N….O and H…..O distances are 2.747 Å and 1.85 Å, respectively. We calculated the bond length of H...O as 1.50 Å. The long bond length in the crystal, as compared with the calculated bond length, may be attributed to the fact that the calculation performed for a single compound in the gaseous state did not involve the intermolecular interactions in the crystal packing. The geometric parameters of rasagiline in the ethandisulfonate salt are not much affected by the presence of the ethanedisulfonate group.

Mesylate is an ester of methanesulfonic acid (MSA, CH_3SO_3H). In salts, the mesylate is present as the $CH_3SO_3^-$ anion. Experimental data on the structure of rasagiline mesylate have not yet been reported. In this work, the equilibrium geometries of rasagiline mesylate (Fig. 3b) were also calculated to assess the influence of the anion on the protonation characteristics of the drug. The crystal structure of sodium [31] and magnesium methanesulfonate [32] has been reported. *Ab initio* calculations have been performed on the structural parameters of monomer methanesulfonic acid (CH_3SO_2OH) in the gas phase [33]. The fully optimized

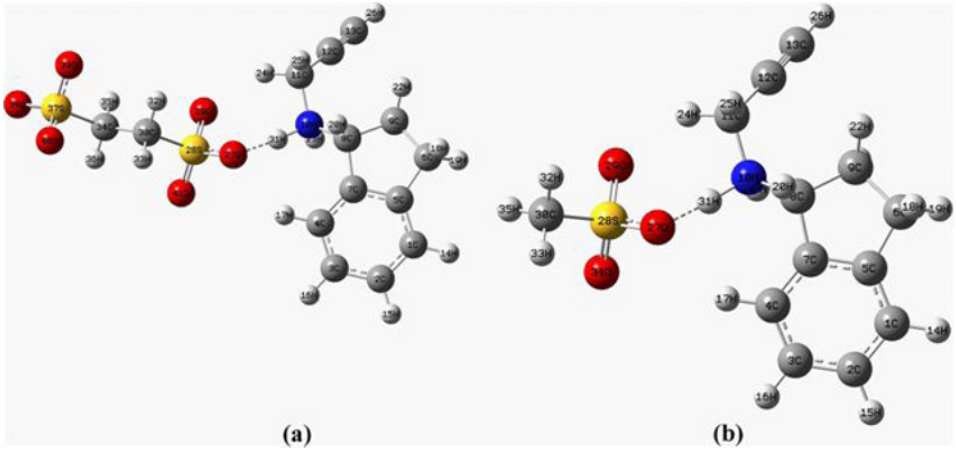

Figure 3. Optimized structures [B3LYP/6-31++G(d,p)] and atom numbering for rasagiline ethanedisulfonate (a) and rasagiline mesylate (b).

geometry of the mesylate anion ($CH_3SO_3^-$) was calculated using DFT/ B3LYP/ 6-31G (d,p) by Tuttolomondo *et al.* [34]. The equilibrium structural parameters (*e.g.* S-O, S-C bond lengths and O-S-O bond angle) calculated for the mesylate anion agree very well with the above-mentioned literature data (Table 2).

Palmer *et al*. [35] studied the crystal structures of the primidine derivatives lamotrigine mesylate salt (used in the treatment of epilepsy) and sipatrigine (which has potent neuroprotective properties). They reported that the oxygen atoms of the CH_3SO_3 solvate ion take part in hydrogen bonding to the NH_2 groups of lamotrigine. The crystal structure of the mesylate salt of lamotrigine is characterized by distinct hydrogen bonding. The crystal structure of sipatrigine (without mesylate) has only one weak hydrogen bond. The bond lengths and bond angles in both compounds are similar. We also expect that the rasagiline cation and mesylate anion are linked by hydrogen bonding in the solid structure. The NH_2^+ groups of rasagiline act as proton donors, thus forming N–H…O hydrogen bonds with the oxygen atoms of mesylate anions. The presence of mesylate and hydrogen bonding in this structure increases the stability of the drug. As shown in Table 2, the geometric parameters of rasagiline in rasagiline mesylate do not change with respect to the rasagiline free base structure.

4. Vibrational analysis

4.1. Rasagiline

The calculated harmonic, anharmonic frequencies and infrared intensities of the most stable conformer (**I**) of rasagiline free base are listed in Table 3 together with the experimental FTIR data obtained from the literature [6].

For approximate characterization of the vibrations, we use the total energy distribution (TED). The last column in the Table 3 contains qualitative mode decomposition for contributions higher than 5%.

The vibrational frequencies of the indane ring [14,36] and propargyl [28,37-40] were also used as guidelines for the assignment of the fundamental vibrational modes of rasagiline.

The solid phase IR spectrum of rasagiline free base was obtained from literature [6]. The experimental (KBr) spectrum of rasagiline free base and theoretical infrared spectra calculated at B3LYP/6-31++G(d,p) theory level for most stable conformer are presented in Fig. 4a and 4b, respectively

In the solid phase infrared spectrum of rasagiline, a narrow band at 3324 cm^{-1} and a medium-broad band at about 3219 cm^{-1} were observed [6]. The B3LYP predicted a frequency of 3526 cm^{-1}, with a predicted intensity of 1.45 km mol^{-1}, and 3479 cm^{-1}, with a predicted intensity of 100 km mol^{-1}, for N-H and propargyl C-H stretching frequency in the gas phase, respectively. The C–H stretch of the C-H bond adjacent to the carbon-carbon triple bond (–C≡C–H) appears as a narrow band in the range 3330-3270 cm^{-1}. In an earlier experiment, the high-frequency acetylenic stretching mode of propargyl radical [38], propargyl amine [29], and propargyl bromide [40] was observed at ca. 3330 cm^{-1}. In contrast to our calculation, we prefer to designate the band at 3324 cm^{-1} in the experimental infrared spectrum (calc. 3479 cm^{-1}) as the ≡C–H stretching mode.

We designated the observed band at 3219 cm^{-1} as the N-H stretching mode in the spectrum of solid rasagiline [6]. Iga *et al*. [14] and Barbu-Debus *et al*. [41] suggested that the stable conformer should be stabilized by intramolecular N-H….π hydrogen bonding between the amino hydrogen and the π-electron of the benzene ring in the aminoindan molecule. We also suggest that

Table 3. Vibrational wavenumbers (cm^{-1}), Total Energy Distributions (TED) and normal mode descriptions of rasagiline.

Mode	Rasagiline				%TED [c] (B3LYP)
	Harmonic	I[a]	Anhar.	Exp.[b]	
1	30	0.11	25		$\tau_{CCNC}(40) + \tau_{HNCC}(28) + \tau_{CNCH}(17)$
2	73	0.13	69		$\tau_{CCNC}(54) + \tau_{HCNC}(24) + \tau_{CCNH}(6) + \delta_{CNC}(6)$
3	96	0.17	89		$\tau_{HCCN}(32) + \tau_{CCCN}(21) + \tau_{CCCC}(12) + \delta_{CNC}(10)$
4	142	2.13	136		$\tau_{CCCH}(25) + \tau_{CCCC}(11) + \tau_{NCCC}(14) + \tau_{HCCC}(12) + \delta_{CCN}(8)$
5	168	0.43	162		$\tau_{CCCH}(29) + \tau_{CCCC}(17) + \delta_{CCN}(10)$
6	209	1.93	205		$\tau_{CCCC}(30) + \text{LİNP}_{CCCH}(14) + \tau_{CCCH}(11)$
7	265	2.93	260		$\tau_{CCCC}(26) + \tau_{HNCH}(14) + \text{LİN}_{CCCN}(12) + \tau_{CCCH}(8) + \tau_{CNCH}(6)$
8	287	3.15	282		$\text{LİNC}_{HCCH}(68) + \text{LİNP}_{CCCN}(18)$
9	345	7.83	329		$\text{LİNC}_{CCCH}(38) + \text{LİNP}_{CCCH}(31)$
10	409	1.38	402		$\tau_{CCCC}(38) + \delta_{CCN}(12) + \tau_{NCCC}(10) + \tau_{CCCH}(22)$
11	437	2.22	430		$\delta_{CCC}(54) + \tau_{CCCH}(26) + \tau_{CCNH}(23)$
12	456	12.30	446	431m	$\tau_{CCCC}(49) + \tau_{CCCH}(22) + \nu CN(5)$
13	520	3.60	510		$\tau_{CCCC}(37) + \tau_{CCCH}(21) + \tau_{HNCC}(15)$
14	522	6.47	514	530w	$\tau_{CCCH}(41) + \tau_{CCCC}(19)$
15	561	27.50	548	547m	$\delta_{CCN}(33) + \tau_{HNCC}(16) + \text{LİNC}_{CCCN}(11) + \text{LİNP}_{CCCH}(6)$
16	610	1.60	600	569m	$\delta_{CCC}(54) + \tau_{CCCH}(23)$
17	627	81.90	627	612m	$\text{LİNC}_{HCCH}(48) + \text{LİNP}_{HCCN}(24) + \text{LİNC}_{CCCH}(13) + \text{LİNP}_{CCCN}(9)$
18	647	8.24	642		$\delta_{CCC}(34) + \text{LİNP}_{CCCH}(28) + \delta_{CNC}(21)$
19	655	85.80	660	669m	$\text{LİNP}_{HCCH}(87)$
20	710	59.90	673	694sbr	$\tau_{CCNH}(49) + \tau_{CCCC}(27)$
21	741	57.40	707	720m	$\tau_{CCNH}(36) + \tau_{CCCC}(31) + \tau_{CCCH}(11)$
22	757	52.90	744	754s	$\tau_{CCCH}(61) + \delta_{CCC}(14)$
23	780	40.30	769	773m	$\tau_{CCCH}(49) + \delta_{CCC}(24)$
24	837	5.24	824	789ms	$\delta_{CCC}(31) + \tau_{CCCH}(22) + \tau_{HCCH}(19)$
25	866	4.32	849	834m	$\tau_{CCCH}(62) + \delta_{CCC}(26)$
26	893	1.16	875	864w	$\tau_{CCCH}(78)$
27	915	33.57	896	900m	$\nu_{CC}(62) + \delta_{CCH}(25) + \delta_{CCN}(12)$
28	950	4.99	933	915s	$\tau_{CCCH}(41) + \tau_{HCCH}(31) + \delta_{CCC}(6)$
29	956	3.92	936	925w	$\tau_{HCCH}(42) + \tau_{HCNC}(24) + \nu_{CN}(15)$
30	964	5.52	945	948w	$\tau_{HCCH}(47) + \delta_{CCC}(16) + \nu_{CC}(12)$
31	980	0.63	957		$\tau_{HCCH}(48) + \delta_{CC8H}(28)$
32	995	0.16	976	993w	$\tau_{CCCH}(87)$
33	1040	14.62	1014	1020m	$\nu_{CC}(37) + \tau_{HCCH}(24) + \nu_{CN}(5)$
34	1046	3.41	1030	1030m	$\nu_{CC}(55) + \delta_{CCH}(27)$
35	1097	2.41	1067		$\delta_{CNC}(39) + \delta_{CCH}(18) + \tau_{HCNH}(12)$
36	1107	12.43	1086		$\delta_{CCH}(33) + \delta_{CCC}(24) + \nu_{CN}(15)$
37	1153	89.17	1124	1079s	$\nu_{CN}(68) + \nu_{CC}(8)$
38	1166	15.39	1139	1091m	$\tau_{CCCH}(32) + \delta_{CCH}(26) + \nu_{CN}(7)$
39	1178	0.84	1158	1152m	$\delta_{CCH}(49) + \nu_{CC}(26)$
40	1180	5.99	1162	1161m	$\delta_{CCH}(64) + \nu_{CC}(21)$
41	1207	1.20	1177	1183m	$\delta_{CCH}(29) + \tau_{CCCH}(24) +) + \nu_{CC}(11) + \tau_{HCCH}(9)$
42	1229	3.040	1202	1207w	$\nu_{CC}(48) + \tau_{CCCH}(22)$
43	1268	11.07	1241	1243m	$\delta_{CCH}(55) + + \tau_{HCCH}(13)$
44	1288	5.87	1257	1257m	$\delta_{CCH}(43) + \tau_{HCCH}(14) + \nu_{CC}(9)$
45	1302	6.47	1268		$\delta_{CCH}(21) + \tau_{CCCH}(18) + \tau_{HCCH}(14) + \nu_{CC}(12)$
46	1321	3.45	1297	1291m	$\delta_{HCC}(23) + \tau_{HCCH}(16) + \tau_{HCCC}(17)$
47	1331	2.06	1299		$\delta_{CCH}(46) + \tau_{HCCC}(23) + \tau_{HCCH}(14)$
48	1362	41.23	1332	1333s	$\delta_{HCN}(37) + \delta_{CCH}(26) + \delta_{NCH}(5)$
49	1368	0.73	1339		$\nu_{CC}(62) + \delta_{CCH}(10)$
50	1383	17.43	1347		$\delta_{HCN}(29) + \delta_{CCH}(16) + \tau_{HCCC}(18) + \delta_{NCH}(11) +$
51	1464	11.19	1435	1429m	$\delta_{HCH}(52) + \tau_{HCNC}(18) + \tau_{HCNH}(18) + \delta_{HCN}(6)$
52	1484	3.85	1447	1447s	$\delta_{HCH}(28) + \tau_{HCCH}(18) + \tau_{HCCC}(14)$
53	1491	4.26	1461	1462mw	$\delta_{CCH}(48) + \nu_{CC}(30)$
54	1501	48.66	1464	1479s	$\delta_{HCH}(23) + \tau_{HCCH}(28) + \delta_{HNC}(13)$

Continued **Table 3.** Vibrational wavenumbers (cm^{-1}), Total Energy Distributions (TED) and normal mode descriptions of rasagiline.

Mode	Rasagiline				%TED [c] (B3LYP)
	Harmonic	I[a]	Anhar.	Exp.[b]	
55	1502	29.62	1472		δ_{HNC} (57) + δ_{HCH} (11)
56	1512	19.15	1474		δ_{CCH} (46) + ν_{CC} (32)+
57	1633	1.50	1595	1586w	ν_{CC} (72)+ δ_{CCH} (9)
58	1652	2.00	1613	1604m	ν_{CC} (68)+ δ_{CCH} (13)
59	2207	2.60	2169	2100m	ν_{CC} (96)
60	2992	35.75	2843	2848m	ν_{CH} (99)
61	3018	51.56	2862	2873s	ν_{CH} (99)
62	3035	40.17	2914		ν_{CH} (100)
63	3048	37.28	2928	2915mw	ν_{CH} (100)
64	3071	15.17	2930	2931m	ν_{CH} (100)
65	3077	46.67	2932	2944s	ν_{CH} (98)
66	3119	47.69	2972	2953ms	ν_{CH} (99)
67	3171	5.49	3008	3025m	ν_{CH} (99)
68	3182	18.39	3030	3046mw	ν_{CH} (100)
69	3195	37.36	3049	3069mw	ν_{CH} (100)
70	3204	28.84	3064	3092mw	ν_{CH} (97)
71	3479	100.00	3354	3324m	ν_{CH}(96)
72	3526	1.45	3359	3219mbr	ν_{NH}(100)

[a] IR intensities (Km mol^{-1}),
[b] Experimental frequencies from IR spectrum in cm^{-1} [6], v = very, s = strong, w = weak, br = broad.
[c] The numbers before the mode symbols indicate % contribution (5 or more) of a given mode to the corresponding normal vibration, according to the TED total energy distribution
Vibrational modes: ν, stretching; δ, deformation; τ, torsion,
LIN C and LINP colinear and coplanar lineer bending code,respectively

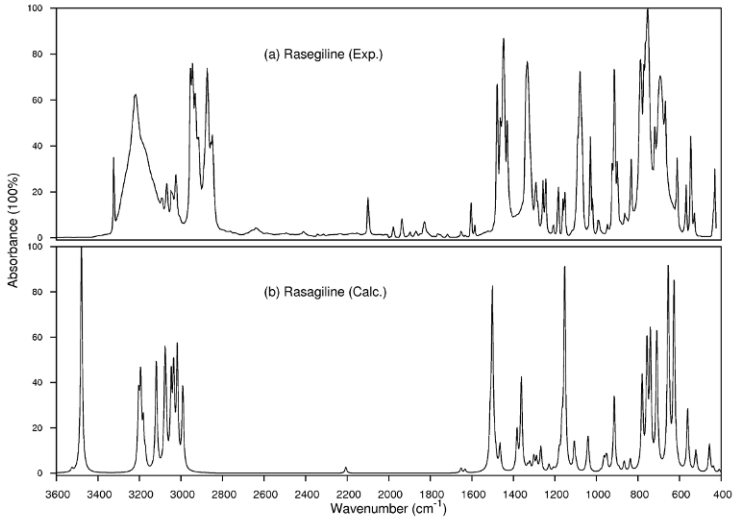

Figure 4. IR spectra of rasagiline (a) The experimental solid phase FT-IR spectrum of rasagiline free base [6] (b) The predicted gas phase IR spectrum computed at B3LYP/6-31++G(d,p) basis set.

the presence of hydrogen bonding results in a shift of the N-H band in the solid structure of rasagiline to lower frequencies.

The propargyl chain has a carbon-carbon triple bond (–C≡C–). The –C≡C– stretch appears as a weak band from 2260-2100 cm^{-1}. The sharp, weak band at 2100 cm^{-1} (calc. 2206 cm^{-1}) is assigned to the stretching vibration of the carbon-carbon triple bond in the infrared spectrum of rasagiline. For propargyl peroxy radical [38], propargyl alcohol [39] and propargyl fluoride [40], the experimental C≡C–H frequencies are reported in the region 690-620 cm^{-1}. From TED, the calculated anharmonic frequencies at 627 cm^{-1} and 660 cm^{-1} are assigned to the C≡C–H out-of-plane and in-plane bending modes, respectively. There are two bands at 669 cm^{-1} and 612 cm^{-1} in the infrared spectrum of rasagiline. These

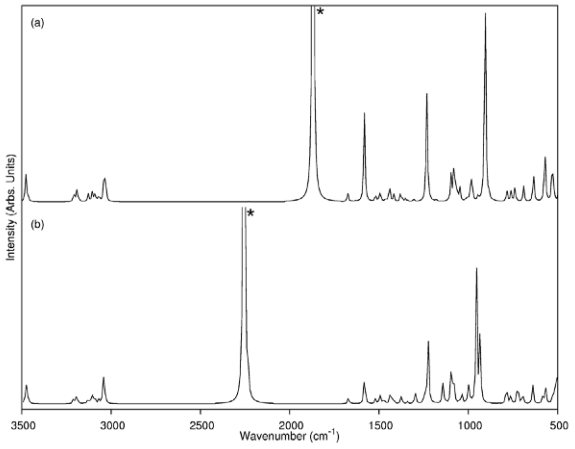

Figure 5. The predicted gas phase IR spectra (a) rasagiline mesylate (b) and rasagiline ethandisulfonate. The calculated N–H…O stretching bands at 2256 cm^{-1} and 1870 cm^{-1} are denoted by*, for rasagiline mesylate and ethandisulfonate, respectively.

bands are tentatively assigned as propargyl C≡C–H in-plane and out-of-plane bending modes, respectively.

The aromatic C-H stretching vibrations appear at 3120 and 3000 cm^{-1}. The experimentally observed bands at 3092, 3069, 3046 and 3025 cm^{-1} in the IR spectrum of rasagiline are assigned to the CH-stretching of phenyl group of rasagiline. The five-membered ring has two methylene groups (CH_2), and the propargyl group has one CH_2 group. Theoretically, three asymmetric CH_2 stretching (ν_a CH_2) and three symmetric (ν_s CH_2) modes are expected in the 2800-3000-cm^{-1} region. The deformations that CH_2 groups undergo include scissoring, wagging, twisting and rocking modes. These modes are distributed over a wide spectral range. All bands of the CH_2 group are assigned using TED and the GaussView 03 W program. The complete assignments of this group and the other modes of rasagiline free base are given in Table 3. There are large shifts between the harmonic frequencies for the fundamentals in the gas phase and those in the solid. It may be observed that the calculated harmonic frequencies require significant scaling to agree with the experimental values. No such scaling is required for the anharmonic frequencies, which are quite close to the experimental values.

4.2. Rasagiline salts

The selected harmonic vibrational frequencies calculated for rasagiline mesylate and rasagiline ethanedisulfonate at the B3LYP level using the 6-31++G (d, p) basis set, assignments, and IR intensities are summarized in Table 4. All other computed frequencies and assignments are given in Table 1.

The previously reported spectra for ethyl methanesulfonate [34] and methanesulfonic acid [33,42] were used as a guide for the assignment of mesylate (methanesulfonate) anion ($CH_3SO_3^-$) bands. The vibrational analysis of disodium 1,2-ethandisulfonate [43] was used as a guide for the assignment of the ethanedisulfonate anion ($O_3SCH_2CH_2SO_3^-$). Previous patent studies provide some IR data and the spectrum of rasagiline mesylate [13] without assignment. No previous study of the experimental infrared spectrum for rasagiline ethandisulfonate was found. The predicted gas-phase infrared spectra of rasagiline mesylate and rasagiline ethandisulfonate are shown in Figs. 5a and 5b, respectively.

There are considerable changes for NH modes in the presence of mesylate/ethandisulfonate anions (Table 4). In our proposed structure (Fig. 3b), methanesulfonic anion and monoprotonated rasagiline are held together by hydrogen bonds. The NH_2^+ group of rasagiline acts as a proton donor, thus forming an N–H…O hydrogen bond. The calculated bands at 3478 cm^{-1} and 1870 cm^{-1} (an intense maximum in Fig. 5a is denoted by *) are assigned as the N–H stretching and N–H…O stretching vibrations, respectively. In the crystal structure of rasagiline ethanedisulfonate, ethanedisulfonate anions ($C_2H_4O_6S_2^-$) are also connected by an N-H….O hydrogen bond to rasagiline cations (Fig. 3a). In this structure, the N–H stretching frequency is calculated to be 3476 cm^{-1}, which is similar to that of rasagiline mesylate. In contrast, the calculated N-H…O frequency is higher than that of rasagiline mesylate (2256 cm^{-1}), which features a longer N-H…O bond (an intense maximum in Fig. 5b is denoted by *). The values calculated for N–H stretching suggest that these bond types have a similar proton-donating ability. The shorter N-H…O bond suggests stronger H-bonding in rasagiline mesylate.

The predicted harmonic frequencies at 3479, 3466 and 3462 cm^{-1} are assigned as C≡C-H stretching for rasagiline, rasagiline mesylate and rasagiline ethandisulfonate, respectively. The observed bands at 3324 cm^{-1} (v ≡C-H) and 3219 cm^{-1}(v N-H) in the infrared spectrum of rasagiline disappeared, and a sharp band at 3278 cm^{-1} appeared in the solid IR spectrum of rasagiline mesylate [13]. We assigned this band to the ≡C-H stretching vibration of propargyl group of rasagiline mesylate. A frequency shift to lower and higher wavenumbers is found for the ≡C-H and the C≡C stretching vibrations of propargyl, respectively, in the experimental and theoretical infrared spectra of rasagiline mesylate (Table 4). These shifts were also found for the calculated frequencies of rasagiline ethandisulfonate. It may be explained by a hydrogen-bonded ≡CH stretching vibration (or no conjugation) in the rasagiline salts. In protonated forms, propargyl CH_2

Table 4. Selected harmonic wave numbers (cm^{-1}) obtained for rasagiline salts at B3LYP/6-31++G(d,p).

Ras. ethandisulfonate	I[a]	Ras. Mesylate[b]	I[a]	Rasagiline	I[a]	Assignment
640	25.54	635 [646]	60.50	655	58.49	δ(≡C-H)
697	42.87	691	44.78	627	55.85	γ (≡CH)
1144	73.27	1080 [1047]	127.54	-	-	ν_s(S=O)
1226	254.85	1232 [1152]	302.27	-	-	ν_a(S=O)
1581	119.98	1583	278.19	-	-	δ (NH..O)
1671	24.44	1676	26.50	1502	20.17	δ(NH)
2233	70.83	2231 [2126]	0.55	2207	2,60	ν(C≡C)
2256	2891.78	1870	2743.95	-	-	ν(NH…O)
3462	21.72	3466 [3278]	18.06	3479	68.13	ν(≡CH)
3476	84.51	3478	81.30	3525	0.98	ν (NH)

[a] *IR intensities (Km mol^{-1}),*
[b] *Observed IR wave numbers [13] are given in bracket*

(which is bonded to the N atom) vibrations are blue-shifted with respect to the rasagiline free base.

4.2.1. Mesylate anion

The calculated bands at 1232 cm^{-1} and 1080 cm^{-1} were assigned to S-O asymmetric and symmetric stretching, respectively. The calculated band at 740 cm^{-1} was assigned as C-S stretching mode. The calculated bands at 531, 495, 489 and 355 cm^{-1} were assigned as SO_3 bending modes. In the solid IR spectrum of rasagiline mesylate [13], the band appears at about 778 cm^{-1}, which may be assigned to C–S stretching. The bands at 1152, 1047 and 540 cm^{-1} may be assigned to the other SO_3 group modes.

The calculated bands at 3180 cm^{-1} and 3076 cm^{-1} were assigned to C-H asymmetric and symmetric stretching modes of the methyl group, respectively. Methyl group deformations are usually observed in the range 1300-1500 cm^{-1}; thus, the calculated frequencies at 1465 and 1353 cm^{-1} were assigned as δ (CH_3) deformation modes.

The methyl and methylene rocking, wagging and twisting vibrations are mechanically coupled to various ring deformation modes (Table 1).

4.2.2. Ethanedisulfonate anion

The ethanedisulfonate anion has two possible conformations: the trans (T) form with *C2h* symmetry and the gauche (G) form with *C2* symmetry. The crystal structure of rasagiline ethandisulfonate [5] has C2 symmetry and displays threefold disorder on the CH_2—CH_2 group. Ohno *et al*. [43] performed vibrational analysis of disodium a,w-alkanedisulfonates, experimentally and theoretically. They used the C-S stretching vibration in the 750-850 cm^{-1} region to determine the conformation of the C-C bond adjacent of the C-S bond. They calculated the C-S stretching frequencies at 750 cm^{-1} (G form), 787 and 811 cm^{-1} (T form). We calculated two bands at 781 and 726 cm^{-1} for the C-S stretching mode. There is no experimental infrared spectrum of solid rasagiline ethandisulfonate in the literature. We propose that the predominant molecular form in the gas phase is the trans conformation about the CC-CS axis.

5. Conclusions

The molecular structure, conformational stability, and vibrational frequencies of rasagiline were investigated using the DFT/ B3LYP/6-31++G(d,p) method. The eight stable conformers were found using a series of B3LYP/6−31++G(d,p) relaxed potential energy scans varying the different dihedrals. Single-point energy calculations were then performed for these conformers at the MP2/6-31++G(d,p) level. The relative single point MP2 energies among conformers are noticeably different from those obtained with DFT. The B3LYP and MP2 calculations were performed with the Gaussian 03 program package. The optimized geometries of the rasagiline, rasagiline mesylate and rasagiline ethandisulfonate were interpreted and compared with the reported experimental values for rasagiline ethandisulfonate. Reasonable agreement between the experimental and computed anharmonic spectra of rasagiline free base was found. Detailed assignment of the fundamental modes of rasagiline was performed based on SQM method. NH and C≡C-H stretching modes of rasagiline are more affected by the mesylate and ethandisulfanate anion than are those of rasagiline free base and these differences was interpreted. We hope that the results of this study will be useful in understanding the spectral properties of other rasagiline salts.

References

[1] J. Jankovic, J. Neurol. Neurosurg. Psychiatry 79, 368 (2008)
[2] M. Yogev-Falach, T. Amit, O. Bar-Am, M.B.H. Youdim, The FASEB Journal 17, 2325 (2003)
[3] S. Li, S. Wong, S. Sethia, H. Almoazen, Y.M. Joshi, A.T.M. Serajuddin, Pharmaceutical Research 22, 628 (2005)
[4] Patent No: US2010/0234636 A1, Novel Salts of the Active Substance Rasagiline, 2010
[5] J. Bruning, J.W. Bats, M.U. Schmidt, Acta Cryst. C 64, o613 (2008)
[6] Patent No: US 2008/0161408 A1 Crystalline Solid Rasagiline base, 2008
[7] G. Rauhut, P. Pulay J. Phys. Chem., 99, 3093 (1995)
[8] J. Baker, A.A. Jarzecki, P. Pulay, J. Phys.Chem. A 102, 1412 (1998)
[9] M.J. Frisch, G.W. Trucks, H.B. Schlegel, G.E. Scuseria, M.A. Robb, J.R. Cheeseman, J.A. Montgomery, Jr., T. Vreven, K.N. Kudin, J.C. Burant, J.M. Millam, S.S. Iyengar, J. Tomasi, V. Barone, B. Mennucci, M. Cossi, G. Scalmani, N. Rega, G.A. Petersson, H. Nakatsuji, M. Hada, M. Ehara, K. Toyota, R. Fukuda, J. Hasegawa, M. Ishida, T. Nakajima, Y. Honda, O. Kitao, H. Nakai, M. Klene, X. Li, J.E. Knox, H.P. Hratchian, J.B. Cross, C. Adamo, J. Jaramillo, R. Gomperts, R.E. Stratmann, O. Yazyev, A.J. Austin, R. Cammi, C. Pomelli, J.W. Ochterski, P.Y. Ayala, K. Morokuma, G.A.Voth, P. Salvador, J.J. Dannenberg, V.G. Zakrzewski, S. Dapprich, A.D. Daniels, M.C. Strain, O. Farkas, D.K. Malick, A.D. Rabuck, K. Raghavachari, J.B. Foresman, J.V. Ortiz, Q. Cui, A.G. Baboul, S. Clifford, J. Cioslowski, B.B. Stefanov, G. Liu, A. Liashenko, P. Piskorz, I. Komaromi, R.L. Martin, D.J. Fox, T. Keith, M.A. Al- Laham, C.Y. Peng, A. Nanayakkara, M. Challacombe, P.M.W. Gill, B. Johnson, W. Chen, M.W. Wong, C. Gonzalez, J.A. Pople, GAUSSIAN 03, Revision B. 04 (Gaussian, Inc., Pittsburgh PA, 2003)
[10] C. Lee, W Yang, R.G. Parr, Phys. Rev. B 37,785 (1988)
[11] A.D. Becke, J. Chem. Phys. 98, 5648 (1993)
[12] SQM version 1.0 (Parallel Quantum Solutions, Fayetteville, AR 72703) http://www.pqs-chem.com.
[13] Patent No: WO 2009 118657A2 Polymorphic Form of an Aminoindan Mesylate Derivative, Publication Date 01.10.2009
[14] H. Iga, T. Isozaki, T. Suzuki, T. Ichimura, J. Phys. Chem. A 111, 5981 (2007)
[15] O. Bar-Am, M. Yogev-Falach, T. Amit, Y. Sagi, M.B.H. Youdim, J. Neurochem. 89, 1119 (2004)
[16] A.D. Becke, Phys. Rev. B 38, 3098 (1988)
[17] M.L. Zhang, Z.J. Huang, Z.J. Lin, J. Phys. Chem. A 122, 134313 (2005)
[18] Z.J. Huang, Z.J. Lin, J. Phys. Chem. A 109, 2656 (2005)
[19] M.J. Frisch, M. Head-Gordon, J.A. Pople, Chem. Phys. Lett. 166,275 (1990)
[20] P.R. Schreiner, Angew. Chem. Int. Ed. 46, 4217(2007)
[21] S. Grimme, J. Comput. Chem. 25, 1463 (2004)
[22] J.E. Rode, J.Cz. Dobrowolski, J. Sadlej, J. Mol. Model. 17, 961 (2011)
[23] J. Rak, P. Skurski, J. Simons, M. Gutowski, J. Am. Chem. Soc. 123, 11695 (2001)
[24] B. Boeckx, R. Ramaekers, G. Maes, Biophysical Chemistry 159, 247 (2011)
[25] A.E Shields, T. Van Mourik, J. Phys. Chem. A 111, 13272 (2007)
[26] T. van Mourik. Chem. Phys. 304, 317 (2004)
[27] S. Scheiner, Hydrogen Bonding. A Theoretical Perspective (Oxford University Press, New York, 1997)
[28] K.M. Marstokk, H. Møllendal, Acta Chemica Scandinavica A 39, 483 (1985)
[29] G.A. Guirgis, S. Bell, C. Zheng, J.R. Durig, Phys. Chem. Chem. Phys. 4, 1438 (2002)
[30] K.-H. Wiedenmann, I. Botskor, H.-D. Rudolph, J. Mol. Spectrosc. 113, 186 (1985)
[31] C.H. Wei, B.E. Hingerty, Acta Cryst. B 37, 1992 (1981)
[32] F.E. Genceli-Guner, M. Lutz, T. Sakurai, A.L. Spek, T. Hondoh, Crystal Growth & Design 10, 4327 (2010)
[33] J.R. Durig, L. Zhou, T. Schwartzt, T. Gounev, J. Raman Spectrosc. 31, 193 (2000)
[34] M.E. Tuttolomondo, A. Navarro, T. Peña, E.L. Varetti, A. Ben Altabef, J. Phys. Chem. A 109, 7946 (2005)
[35] R.A. Palmer, B.S. Potter, M.J. Leach, B.Z. Chowdhry, J. Chem. Crystallogr. 37,771 (2007)
[36] J. Oomens, G. Meijer, G.von Helden, J. Phys. Chem. A 105, 8302 (2001)
[37] T. Gilbert, R. Pfab, I. Fischer, P. Chen, J. Chem. Phys. 112, 2575 (2000)
[38] E.B. Jochnowitz, X. Zhang, M.R. Nimlos, B.A. Flowers, J.F. Stanton, G.B. Ellison, J. Phys. Chem. A. 114, 1498 (2010)
[39] E.L. Stewart, U. Mazurek, J.P. Bowen, J. Phys. Org. Chem. 9, 66 (1996)

[40] J.C. Evans, R.A. Nyquist, Spectrochim. Acta 19, 1153 (1963)
[41] K. Le Barbu-Debus, F. Lahmani, A. Zehnacker-Rentien, N. Guchhait, Phys. Chem. Chem. Phys. 8, 1001 (2006)
[42] A. Givan, A. Loewenschuss, C.J. Nielsen, J. Mol. Struct. 748, 77 (2005)
[43] K. Ohno, T. Naganobu, H. Matsuura, H. Tanaka, J. Phys. Chem. 99, 8477 (1995)